AKADÉMIAI KIADÓ

Resolution and Discovery

6 (2021) 1, 25–31

DOI:
10.1556/2051.2022.00093

ORIGINAL RESEARCH PAPER

Quantitative dSTORM superresolution microscopy

TIBOR NOVÁK[1], DÁNIEL VARGA[1], PÉTER BÍRÓ[1], BÁLINT BARNA H. KOVÁCS[1], HAJNALKA MAJOROS[2,3,4], TIBOR PANKOTAI[2,3,4], SZILÁRD SZIKORA[5], JÓZSEF MIHÁLY[5,6] and MIKLÓS ERDÉLYI[1*]

[1] Department of Optics and Quantum Electronics, University of Szeged, 9 Dóm tér, H-6720 Szeged, Hungary

[2] Institute of Pathology, Albert Szent-Györgyi Medical School, University of Szeged, 1 Állomás utca, H-6725 Szeged, Hungary

[3] Centre of Excellence for Interdisciplinary Research, Development and Innovation, University of Szeged, 13 Dugonics tér, H-6720 Szeged, Hungary

[4] Hungarian Centre of Excellence for Molecular Medicine (HCEMM)–University of Szeged Genome Integrity and DNA Repair Group, 9 Budapesti út, H-6728 Szeged, Hungary

[5] Institute of Genetics, Biological Research Centre, Hungarian Academy of Sciences, Szeged, Hungary

[6] Department of Genetics, University of Szeged, 52 Közép fasor, H-6726 Szeged, Hungary

Received: December 22, 2021 • Accepted: October 3, 2022
Published online: November 21, 2022

ABSTRACT

Localization based superresolution technique provides the highest spatial resolution in optical microscopy. The final image is formed by the precise localization of individual fluorescent dyes, therefore the quantification of the collected data requires special protocols, algorithms and validation processes. The effects of labelling density and structured background on the final image quality were studied theoretically using the TestSTORM simulator. It was shown that system parameters affect the morphology of the final reconstructed image in different ways and the accuracy of the imaging can be determined. Although theoretical studies help in the optimization procedure, the quantification of experimental data raises additional issues, since the ground truth data is unknown. Localization precision, linker length, sample drift and labelling density are the major factors that make quantitative data analysis difficult. Two examples (geometrical evaluation of sarcomere structures and counting the γH2AX molecules in DNA damage induced repair foci) have been presented to demonstrate the efficiency of quantitative evaluation experimentally.

KEYWORDS

superresolution microscopy, localization method, quantitative imaging, cluster analysis

1. INTRODUCTION

The spatial resolution of optical imaging systems is limited by the diffraction of light [1]. If optical aberrations are neglected and only the diffraction limits the image quality, the resolution can be given with the Rayleigh criterion ($R = 0.61 \cdot \lambda/\mathrm{NA}$, where λ is the wavelength and NA is the numerical aperture) [1]. Due to such a resolution barrier, traditional fluorescence microscopy methods cannot reveal structures below 200 nm, precluding the study of biochemical processes at the single-molecule level. Superresolution methods such as Stimulated Emission Depletion (STED) [2], Structured Illumination (SIM) [3] and Single Molecule Localization Microscopy (SMLM) [4, 5] have been developed to address this issue. Applicability, efficiency and advantages of these methods have been proven in the last years

Based on invited lecture presented at the HSM 2021 Conference.

*Corresponding author.
E-mail: erdelyi.miklos@szte.hu

and they have become "must-have" systems in all modern microscope labs or core facilities. However, after the first positive impressions, attention turns to deeper interpretation of superresolved images. Researchers aim to quantify the results, determine merit functions, correlate them with other techniques and extend their applicability to in vivo measurements. Single molecule localization methods provide a special form of data: a table of coordinates, number of photons, ellipticity, localization precision and other parameters of the localized single molecules. This kind of data architecture is ideal for cluster analysis [6, 7] and molecule counting [8, 9], but pattern recognition [10] and segmentation [11] require new approaches. Quantitative evaluations were used for the ligand-specific dimer formation of TLR4 receptors [12], the characterization of individual vesicles [13], the cluster formation of TNRF1 receptors [14] or the mapping of the sarcomeric H-zone and I-band complexes of indirect flight muscles (IFMs) of Drosophila melanogaster [15]. There are algorithms specifically written for system simulations [16, 17], molecule localizations [18], and the quantitative evaluation [19] of SMLM images. However, the precision and accuracy of the developed methods are typically validated by ground truth datasets. Therefore, in the first part of this paper a simulation code referred to as TestSTORM [20, 17] is shortly discussed. In the second part two examples are presented for quantitative SMLM. In the first example, the substructure of sarcomeres is mapped at <10 nm spatial resolution, while in the second one DNA damage induced repair foci are evaluated by means of cluster analysis.

2. SIMULATIONS

The final image quality in SMLM strongly depends on the sample, the system and the imaging parameters. An artefact-free image requires the intense optimization of a great number of parameters. The experimental optimization procedure is expensive and time consuming, but simulations can provide a quick and effective alternative solution. Presently, there are a few software tools specifically developed for such purposes [16, 17]. In TestSTORM one can set practically all the critical parameters, such as labelling density, linker length and orientation, structured background, exposure time, and drift. The user can also choose the appropriate PSF model (scalar or vector diffraction) and introduce astigmatism for 3D simulations [21]. By changing the parameters one can generate a process window and determine the sensitivity of the final image quality to such parameters. To prove the applicability and advantages of the code, the effect of the labelling density and the structured background will be presented here.

Image stacks were generated by TestSTORM, and superresolved images were reconstructed by rainSTORM [22, 23]. Figure 1 depicts the final images of two parallel lines using different labelling density. The length and separation of the lines were 1,000 nm and 130 nm, respectively. The photophysical constants (ON/OFF time, bleaching rate etc.) of the Alexa Fluor 647 dye was applied during the simulations. Figure 1 shows image degradation with increasing labelling density. The higher the labelling density, the lower the contrast. The red curves show the fitted double Gaussian distributions to the measured data equalling the convolution of the fluorescence dye distribution and the localization precision. The black curves show the fluorescence dye distribution after the deconvolution step. During the simulations, the labelling density changed between 50 and 800 molecule/μm, but it was homogeneous on a single sample.

The chance of the spatial and temporal overlap of active fluorescence molecules increases at high labelling density, which introduces two types of artefacts: the false localization density between the two lines increases and hot spots are formed at the ends of the lines [20]. The first feature is caused by molecules with overlapping PSFs on adjacent lines, whose spots are localized between the true positions of the emitters. The second artefact is the result of reduced

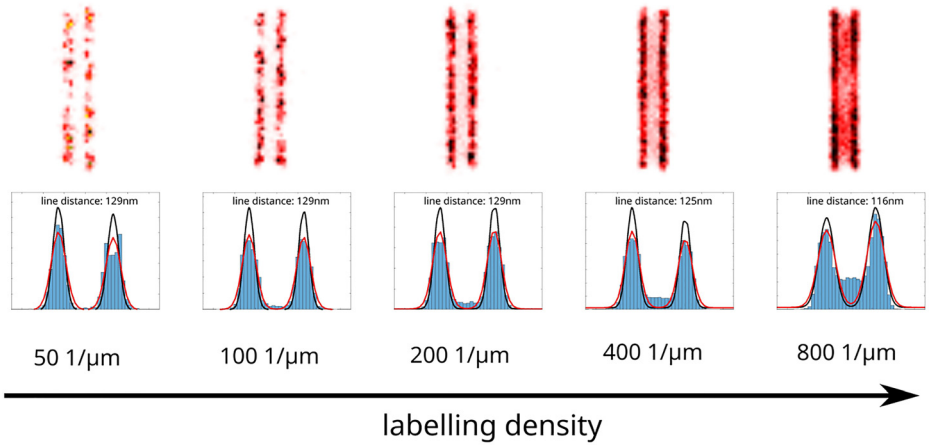

Fig. 1. Reconstructed SMLM images of two parallel lines separated by 130 nm. The labelling density was changed between 50 and 800 molecules per μm

localization density in the middle. Molecules on the midsection of the line overlap with higher probability than those on the edges, and the localization algorithm discards their spots with higher propensity. The PSF overlaps can also reduce the determined separation of the two lines by >10% at high labelling densities (Fig. 1). Technically, the labelling density can be set via the concentration of primary and secondary antibodies. If the final density is low, the measurement takes too long and drift artefact can reduce the image quality. In the opposite case, when the density is high, photobleaching must be applied before SMLM data acquisition to reduce the number of active molecules and decrease the probability of overlaps.

Structured background is another potential source of image degradation in SMLM [17]. Autofluorescence, defocused molecules, or nonspecific labelling can introduce such a static, sample specific background with feature sizes comparable to that of the PSFs. When a molecule emits on such a highly inhomogeneous background, its centre, determined by the localization algorithm, shifts towards the higher intensity region and hence distorts the superresolved images. In Fig. 2, the separation of the two lines was reduced by almost 40% (from 130 to 81 nm) and the shape of the lines was also distorted and became curved. However, the background did not affect the image contrast significantly. The fluorescence background can typically be reduced by using appropriate illumination methods (EPI, HILO, TIRF). Moreover, a postprocessing algorithm estimating and removing the structured background can also be applied [24].

3. EXPERIMENTAL DETAILS

Superresolution images were captured essentially as described previously [15, 25]. Briefly, all dSTORM images were captured under EPI illumination (Nikon CFI Apo 100x, NA = 1.49) on a custom-made inverted microscope based on a Nikon Eclipse Ti-E frame. The laser (MPB Communications Inc.: 647 nm, P_{max} = 300 mW) intensity was set to 2–4 kW cm^{-2} on the sample plane via an acousto-optic tuneable filter (AOTF). An additional laser (Nichia: 405 nm, P_{max} = 60 mW) was used for reactivation. Images were captured by an Andor iXon3 897 BV EMCCD digital camera (512 × 512 pixels with 16 µm pixel size). Frame stacks for dSTORM superresolution imaging were captured at a reduced image size. A fluorescence filter set (Semrock, LF405/488/561/635-A-000) with an additional emission filter (AHF, 690/70 H Bandpass) was used to select and separate the excitation and emission lights in the microscope. During the measurements, the perfect focus system of the microscope was used to keep the sample in focus with a precision of <30 nm. Right before the measurement, the storage buffer of the sample was replaced with a GLOX switching buffer [26] and the sample was mounted onto a microscope slide. Typically, 20,000 to 50,000 frames were captured with an exposure time of 20 or 30 ms. The captured and stored image stacks were evaluated and analyzed with the rainSTORM localization software [22, 23]. Individual images of single molecules were fitted with a Gaussian point-spread function and their central positions were associated with the position of the fluorescent molecule. Localizations were filtered via their intensity, precision and standard deviation values. Mechanical drift introduced by either the mechanical movement of the sample or thermal effects was analyzed and reduced by means of a correlation based blind drift correction algorithm. Spatial coordinates of the localized events were stored and the final superresolved image was visualized.

4. QUANTIFICATION OF DSTORM IMAGES

Superresolved SMLM images can reveal structures in the <10 nm range. The qualitative evaluation of such images has already provided lots of new information and reveals previously unknown details [27]. However, scientists are aiming to quantify the measured data by applying merit functions

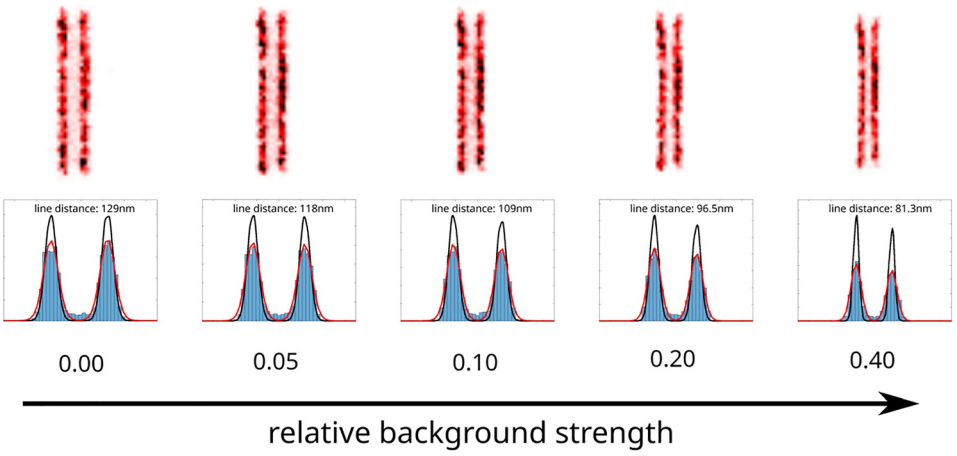

Fig. 2. Reconstructed SMLM images of two parallel lines separated by 130 nm as a function of static structured fluorescence background

and statistical values. Two examples for quantitative evaluation will be shortly discussed in this section. In the first example, the geometrical parameters of the highly ordered sarcomere structure, while in the second one the number of γH2AX histone molecules in DNA damage induced repair foci were evaluated.

4.1. Geometrical evaluation

Indirect flight muscles of Drosophila are complex and extremely highly organized structures made up of hundreds of different proteins. Superresolution dSTORM proved to be an ideal method to examine the substructure of sarcomeres. More than thirty key proteins (tropomodulin, kettin, SALS, DAAM, obscurin, troponin etc.) were labelled individually and their positions were determined with a precision of <10 nm [15, 28]. Figure 3A shows the conventional EPI fluorescence image of flight muscle sarcomeres stained for tropomodulin. The position of the H-zones can be clearly seen, however the double line substructure can only be recognized in the dSTORM superresolved images (Fig. 3A). Quantitative evaluation (determination of the separation of the two lines) requires several post-processing steps. First, the ROIs must be segmented and the central line of the structure has to be found (Fig. 3. B and C). The distance of the localizations from the fitted central curve can be depicted on a histogram (Fig. 3D) and the measured density distribution can be fitted with a theorical curve. For a more realistic sample parameter extraction this fitted curve is deconvolved by the localization precision and the linker length (Fig. 3E). Due to the highly ordered and periodic feature of the sarcomeres, an averaging method (Fig. 3F) can be used to enhance the spatial resolution further. Typically, the positions of the labelled proteins can be determined with a precision of <10 nm via averaging a few hundred sarcomeres, and the measured positions can be used to reconstruct the molecular structure of the sarcomere.

4.2. Molecule counting

Besides the geometrical description, the number of labelled molecules can also provide valuable information on the sample. SMLM seems to be an ideal method for molecule counting, since each accepted localization can be assigned to a single dye molecule. However, in the standard immunohistochemical staining procedure the labelling stoichiometry is typically unknown [29], and the actual number of dye molecules bound to the target molecule can change in a wide range. Therefore, the number of accepted localizations belonging to a single target molecule (the response function of dSTORM imaging) is not deterministic. This value depends on the number of the primary and secondary antibodies, the number of dye molecules, the ratio of the exposure time and the ON-state lifetime, and the number of reactivation cycles. These parameters are usually unknown and are affected by the local chemical environment of the dye molecule. Therefore, an *in situ* data acquisition and

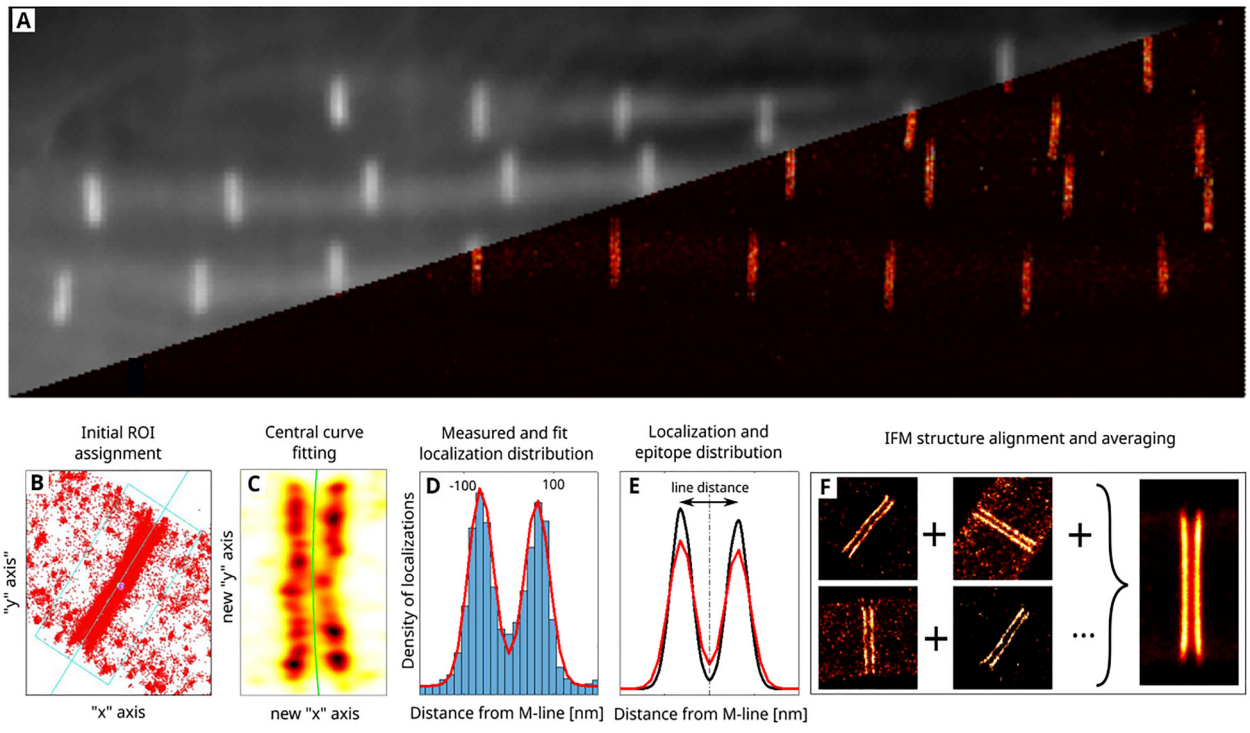

Fig. 3. Conventional EPI and dSTORM (A) images of AF647 labelled tropomodulin in flight muscle sarcomeres. Main steps of data processing: segmentation of ROIs (C), orientation and line shape fitting (D), rough intensity fitting (D) and deconvolution (E). Due to the periodic structure, individual images can be averaged to increase the precision (F)

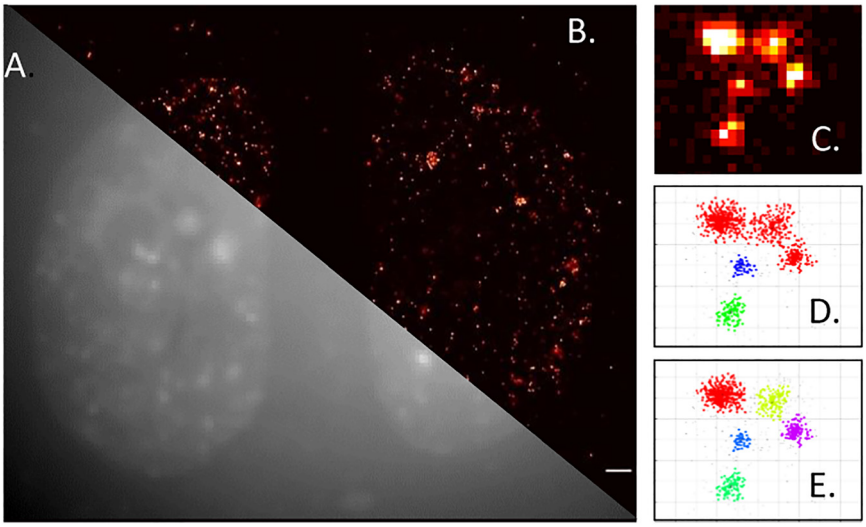

Fig. 4. Epifluorescence (A) and dSTORM superresolved (B) images of AF647 labelled γH2AX. The nanofoci inside the DNA damage induced repair focus (C) were separated by means of 2D (D) and 3D (E) cluster analysis

evaluation method is preferred as described previously [25]. During such a procedure, the ON-state lifetime of individual dyes was determined by trajectory fitting algorithms [23], while the bleach rate and the average number of switching cycles were determined by fitting the theoretical curve to the measured data. Isolated labelled single target molecules were first selected via cluster analysis to determine the response function of the system.

The developed approach was tested for quantifying the DNA damage induced γH2AX foci formation [25] in different cell cultures after neocarzinostatin and 4-Hydroxy-tamoxifen treatments. The substructure of the repair foci that formed could be revealed by dSTORM imaging and the 20–60 nm nanofoci (Fig. 4B, C) were individually characterized. The foci and nanofoci that formed were categorized by their size, area, and the number of labelled γH2AX histone molecules. Their spatial distribution inside the nucleus could also be evaluated and visualized. It was proved that cluster density had not varied in space and showed a homogenous distribution inside the nucleus 2 h after the treatment.

Ionizing radiation, such as X-ray can also induce double-strand breaks. Confocal imaging is a simple and widely used method to follow the formation of γH2AX foci. However, the limited spatial resolution of confocal imaging precludes quantitative evaluation, because at high exposure dose the focus density is too high and therefore cluster analysis is not feasible. Localization data can be used to separate the nanofoci and open the way to quantitative evaluation [30]. However, the number of captured dSTORM images is limited. The applied switching buffer can typically work for 3–4 h, and the entire data acquisition time of an image (selection of ROI, capturing reference images, setting the laser intensity and filters, capturing image stack etc.) is around 10 min. In contrast, a large number of cells can be captured with a confocal microscope during the same time period. Therefore, if statistical evaluation is necessary, correlative measurements (when the advantages of different techniques are combined) are a possible solution.

5. DISCUSSION AND CONCLUSION

Localization based superresolution methods detect and localize individual fluorescence molecules and improve spatial resolution. SMLM provides the x, y and z co-ordinates, the localization precision, ellipticity and other parameters of the images of individual fluorescence molecules (PSF). Such data format can be used for advanced quantitative image analysis. When periodic or highly ordered structures are imaged (sarcomere, nuclear pore complex etc.), the resolution can be further improved by an averaging method. This process requires an automatic segmentation and image registration algorithm. The localization precision and the length of the linker also reduce the image quality. Accurate localization of the labelled target molecule requires deconvolution. The number of labelled molecules of complex structures formed by identical localizations can also be determined. However, the stoichiometry of labelling is typically unknown and the local chemical environment of fluorescence molecules strongly affects the photophysical parameters (ON-state lifetime etc.). Therefore, the response function of dSTORM imaging is not deterministic, the number of target molecules can be determined statistically. The validation of new algorithms, the study of imaging artifacts, and the optimization of imaging parameters requires a test platform. The TestSTORM code was developed and tested for such purposes. The implemented methods made the simulated data more realistic, providing a useful tool to optimize the critical imaging parameters and understand the origin of different imaging artefacts.

ACKNOWLEDGMENTS

This work was supported by the Hungarian Brain Research Program (2017-1.2.1-NKP-2017-00002), the National Research, Development and Innovation Office (TKP2021-NVA-19), the Prime Minister's Office (NTP-NFTÖ-21-B-0197 to DV), and OTKA K132782 (to JM) and OTKA FK138894 (to SS). This research was also funded by the National Research, Development and Innovation Office grant GINOP-2.2.1-15-2017-00052 and NKFI-FK 132080, 2019-1.1.1-PIACI-KFI-2019-00080, the János Bolyai Research Scholarship of the Hungarian Academy of Sciences BO/27/20, ÚNKP-22-5-SZTE-318. The project has received funding from the EU's Horizon 2020 research and innovation program under grant agreement No. 739593. "Project no. TKP-2021-EGA-05 has been implemented with the support provided by the Ministry of Culture and Innovation of Hungary from the National Research, Development and Innovation Fund, financed under the TKP2021-EGA funding scheme."

REFERENCES

1. Born, M.; Wolf, E. *Principles of Optics: Electromagnetic Theory of Propagation, Interference and Diffraction of Light*, 6th ed.; Pergamon Press Ltd.: Oxford, **1986**; pp. 414–8.
2. Klar, T. A.; Jakobs, S.; Dyba, M.; Egner, A.; Hell, S. W. Fluorescence microscopy with diffraction resolution barrier broken by stimulated emission. *Proc. Natl. Acad. Sci.* **2000**, *97*(15), 8206–10.
3. Gustafsson, M. G. L. Surpassing the lateral resolution limit by a factor of two using structured illumination microscopy. Short communication. *J. Microsc.* **2000**, *198*(2), 82–7.
4. Betzig, E.; Patterson, G. H.; Sougrat, R.; Lindwasser, O. W.; Olenych, S.; Bonifacino, J. S.; Davidson, M. W.; Lippincott-Schwartz, J.; Hess, H. F. Imaging intracellular fluorescent proteins at nanometer resolution. *Science* **2006**, *313*(5793), 1642–5.
5. Rust, M. J.; Bates, M.; Zhuang, X. Sub-diffraction-limit imaging by stochastic optical reconstruction microscopy (STORM). *Nat. Methods* **2006**, *3*(10), 793–6.
6. Nicovich, P. R.; Owen, D. M.; Gaus, K. Turning single-molecule localization microscopy into a quantitative bioanalytical tool. *Nat. Protoc.* **2017**, *12*(3), 453–60.
7. Khater, I. M.; Nabi, I. R.; Hamarneh, G. A review of super-resolution single-molecule localization microscopy cluster analysis and quantification methods. *Patterns* **2020**, *1*(3), 100038.
8. Nino, D.; Rafiei, N.; Wang, Y.; Zilman, A.; Milstein, J. N. Molecular counting with localization microscopy: a Bayesian estimate based on fluorophore statistics. *Biophysical J.* **2017**, *112*(9), 1777–85.
9. Hummer, G.; Fricke, F.; Heilemann, M. Model-independent counting of molecules in single-molecule localization microscopy. *Mol. Biol. Cell* **2016**, *27*(22), 3637–44.
10. Peters, R.; Griffié, J.; Burn, G. L.; Williamson, D. J.; Owen, D. M. Quantitative fibre analysis of single-molecule localization microscopy data. *Scientific Rep.* **2018**, *8*(1).
11. Wollman, A. J. M.; Leake, M. C. Millisecond single-molecule localization microscopy combined with convolution analysis and automated image segmentation to determine protein concentrations in complexly structured, functional cells, one cell at a time. *Faraday Discuss.* **2015**, *184*, 401–24.
12. Krüger, C. L.; Zeuner, M.-T.; Cottrell, G. S.; Widera, D.; Heilemann, M. Quantitative single-molecule imaging of TLR4 reveals ligand-specific receptor dimerization. *Sci. Signaling* **2017**, *10*(503).
13. Puchner, E. M.; Walter, J. M.; Kasper, R.; Huang, B.; Lim, W. A. Counting molecules in single organelles with superresolution microscopy allows tracking of the endosome maturation trajectory. *Proc. Natl. Acad. Sci.* **2013**, *110*(40), 16015–20.
14. Weinelt, N.; Karathanasis, C.; Smith, S.; Medler, J.; Malkusch, S.; Fulda, S.; Wajant, H.; Heilemann, M.; Wijk, S. J. L. Quantitative single-molecule imaging of TNFR1 reveals zafirlukast as antagonist of TNFR1 clustering and TNFα-induced NF-κB signaling. *J. Leukoc. Biol.* **2020**, *109*(2), 363–71.
15. Szikora, S.; Gajdos, T.; Novák, T.; Farkas, D.; Földi, I.; Lenart, P.; Erdélyi, M.; Mihály, J. Nanoscopy reveals the layered organization of the sarcomeric H-zone and I-band complexes. *J. Cell Biol.* **2019**, *219*(1).
16. Venkataramani, V.; Herrmannsdörfer, F.; Heilemann, M.; Kuner, T. SuReSim: simulating localization microscopy experiments from ground truth models. *Nat. Methods* **2016**, *13*(4), 319–21.
17. Novák, T.; Gajdos, T.; Sinkó, J.; Szabó, G.; Erdélyi, M. TestSTORM: versatile simulator software for multimodal super-resolution localization fluorescence microscopy. *Scientific Rep.* **2017**, *7*(1).
18. Sage, D.; Pham, T.-A.; Babcock, H.; Lukes, T.; Pengo, T.; Chao, J.; Velmurugan, R.; Herbert, A.; Agrawal, A.; Colabrese, S.; Wheeler, A.; Archetti, A.; Rieger, B.; Ober, R.; Hagen, G. M.; Sibarita, J.-B.; Ries, J.; Henriques, R.; Unser, M.; Holden, S. Super-resolution fight club: assessment of 2D and 3D single-molecule localization microscopy software. *Nat. Methods* **2019**, *16*(5), 387–95.
19. Sage, D.; Kirshner, H.; Pengo, T.; Stuurman, N.; Min, J.; Manley, S.; Unser, M. Quantitative evaluation of software packages for single-molecule localization microscopy. *Nat. Methods* **2015**, *12*(8), 717–24.
20. Sinkó, J.; Kákonyi, R.; Rees, E.; Metcalf, D.; Knight, A. E.; Kaminski, C. F.; Szabó, G.; Erdélyi, M. TestSTORM: simulator for optimizing sample labeling and image acquisition in localization based super-resolution microscopy. *Biomed. Opt. Express* **2014**, *5*(3), 778–87.
21. Huang, B.; Wang, W.; Bates, M.; Zhuang, X. Three-dimensional super-resolution imaging by stochastic optical reconstruction microscopy. *Science (New York, N.Y.)* **2008**, *319*(5864), 810–3.
22. Rees, E. J.; Erdelyi, M.; Schierle, G. S. K.; Knight, A.; Kaminski, C. F. Elements of image processing in localization microscopy. *J. Opt.* **2013**, *15*(9), 094012.
23. rainSTORM software download page. https://titan.physx.u-szeged.hu/~adoptim/?page_id=582 (accessed Dec 07, 2021).
24. Hoogendoorn, E.; Crosby, K. C.; Leyton-Puig, D.; Breedijk, R. M. P.; Jalink, K.; Gadella, T. W. J.; Postma, M. The fidelity of stochastic single-molecule super-resolution reconstructions critically depends upon robust background estimation. *Scientific Rep.* **2014**, *4*(1), 3854.
25. Varga, D.; Majoros, H.; Ujfaludi, Z.; Erdélyi, M.; Pankotai, T. Quantification of DNA damage induced repair focus formation via super-resolution DSTORM localization microscopy. *Nanoscale* **2019**, *11*(30), 14226–36.
26. van de Linde, S.; Löschberger, A.; Klein, T.; Heidbreder, M.; Wolter, S.; Heilemann, M.; Sauer, M. Direct stochastic optical

reconstruction microscopy with standard fluorescent probes. *Nat. Protoc.* **2011**, *6*(7), 991–1009.
27. Huang, B.; Babcock, H.; Zhuang, X. Breaking the Diffraction barrier: super-resolution imaging of cells. *Cell* **2010**, *143*(7), 1047–58.
28. Szikora, S.; Novák, T.; Gajdos, T.; Erdélyi, M.; Mihály, J. Super-resolution microscopy of drosophila indirect flight muscle sarcomeres. *Bio-Protocol* **2020**, *10*(12), e3654.
29. Grußmayer, K. S.; Kurz, A.; Herten, D.-P. Single-molecule studies on the label number distribution of fluorescent markers. *ChemPhysChem* **2014**, *15*(4), 734–42.
30. Brunner, S.; Varga, D.; Bozó, R.; Polanek, R.; Tőkés, T.; Szabó, E. R.; Molnár, R.; Gémes, N.; Szebeni, G. J.; Puskás, L. G.; Erdélyi, M.; Hideghéty, K. Analysis of ionizing radiation induced DNA damage by superresolution DSTORM microscopy. *Pathol. Oncol. Res.* **2021**, 27.